NASA Technical Memorandum 84623

Flow Visualization of the Wake of a Transport Aircraft Model With Lateral-Control Oscillations

Frank L. Jordan, Jr.

JUNE 1983

ERRATA

NASA Technical Memorandum 84623

FLOW VISUALIZATION OF THE WAKE OF A TRANSPORT AIRCRAFT
WITH LATERAL-CONTROL OSCILLATIONS

Frank L. Jordan, Jr.

June 1983

In the original printing, the photographs in figure 5(b). page 16, were inadvertently placed upside down. Please substitute this corrected copy for the original copy.

ISSUE DATE: July 1983

NASA Technical Memorandum 84623

Flow Visualization of the Wake of a Transport Aircraft Model With Lateral-Control Oscillations

Frank L. Jordan, Jr.
Langley Research Center
Hampton, Virginia

National Aeronautics
and Space Administration

**Scientific and Technical
Information Branch**

1983

SUMMARY

A flow-visualization study has been conducted in the Langley Vortex Research Facility to investigate effects of lateral control-surface oscillations on the wake of a 0.03-scale model of a wide-body jet transport aircraft. Effects of both asymmetric surface oscillation (control surfaces move as with normal lateral-control inputs) and symmetric surface oscillation (control surfaces move in phase) were compared to effects of fixed deflected flight spoilers. The asymmetric case simulated a flight maneuver which was previously investigated on the transport aircraft during NASA/FAA flight tests and which resulted in substantial wake-vortex attenuation.

The simulated flight maneuver produced a more disorganized wake with less apparent rotary motion than was obtained with either symmetric surface oscillation or fixed deflected flight spoilers. For this asymmetric case, only a small amount of rotary motion remained in the wake-vortex system once roll-up was complete, a finding consistent with results of the flight tests.

Effects of surface oscillation on the vortex roll-up process were complex. With asymmetric oscillation, asymmetric regions were produced wherein part of the vortex system transferred across the wake centerline, merging with the vortex systems on the other side of the wake. This vortex transfer phenomenon is identified as a possible aerodynamic mechanism contributing to the large amount of attenuation observed with asymmetric oscillation.

Wake roll-up both for oscillating control surfaces and for fixed deflected spoilers was not complete for a full-scale downstream distance of approximately 1 n.mi.

INTRODUCTION

The strong wake vortices generated by large commercial jet transport aircraft are a potential upset hazard to smaller aircraft that are following, resulting in terminal area Instrument Flight Rules (IFR) horizontal separation requirements that have contributed to capacity problems at busy airports. For a number of years, the National Aeronautics and Space Administration has been involved in a broad research effort consisting of model tests, flight tests, and theoretical studies to better understand these wake vortices in order to develop aerodynamic means of minimizing their effects (ref. 1).

As part of this effort, flight tests (ref. 2) were conducted on the Boeing 747 configuration to evaluate the effectiveness of statically deflecting various spoiler segments for vortex attenuation. Because spoiler deflection had been shown to be effective in early tests, and represented a relatively simple retrofit, much recent wake-vortex research has been devoted to evaluating this concept (see ref. 3), including flight tests of the more promising configurations. During the tests described in reference 2, additional flights were performed to determine if aircraft maneuvers on final approach would degrade the vortex attenuation obtained by spoiler deflection. This maneuver consisted of rolling the aircraft periodically by oscillating the roll-control wheel nearly full deflection to produce bank angle excursions

of approximately ±7°. In the maneuver, the spoilers and ailerons were oscillated simultaneously, but the spoiler segments involved were uprigged for the neutral condition, causing them to retract on the rising wing and become farther extended on the falling wing. Unexpectedly, both observation and measurements indicated that these lateral-control oscillations resulted in further attenuation of the wake vortex. For instance, the rolling moments induced on a T-37B probe aircraft encountering the vortex during the tests were mostly within its roll-control power. As a result, this wake caused substantially less roll and bank-angle response on the probe aircraft than did the wake attenuated by static spoiler deflection. In fact, the T-37B pilots reported that this wake was essentially free of organized rotary motion and was somewhat comparable to light-to-moderate turbulence at a 3-n.mi. separation (ref. 2). Substantial attenuation this close behind a heavy-class aircraft is significant in view of current separation requirements, which are 4 to 6 n.mi. depending on the size class of aircraft that are following. Although such a maneuver on final approach is obviously not operationally practical, these test results are of considerable interest because of the large amount of attenuation obtained, and because it is believed that an understanding of the flow mechanisms responsible for the attenuation may suggest more practical concepts.

The purpose of the investigation described in this paper was to simulate the flight control inputs on a 0.03-scale model of the Boeing 747 and to study the effects on the wake in order to obtain some understanding of the flow interactions involved in the wake attenuation. The investigation was exploratory and qualitative in nature, utilizing flow visualization to estimate the amount of attenuation obtained and to study the details of the wake-flow interactions. The investigation was conducted in the Langley Vortex Research Facility.

SYMBOLS

b	wing span, m
C_L	lift coefficient, $\frac{\text{Lift}}{qS}$
c	chord, m
$\bar{c}$	wing mean aerodynamic chord, m
IB	inboard
OB	outboard
q	free-stream dynamic pressure, Pa
S	wing area, m^2
T.E.	trailing edge
x	downstream separation distance, km (n.mi.)

APPARATUS AND PROCEDURES

Test Facility

A sketch of the Langley Vortex Research Facility is shown in figure 1. This facility was developed during the past decade specifically to study the lift-induced vortex flows associated with heavy transport aircraft. A particular feature of the facility is that the aircraft model is towed through the test area rather than being held fixed as in conventional wind tunnels. This feature permits observation of the model-generated wake for long time periods after model passage, which represents large downstream distances.

The facility is 550 m long and has an enclosed overhead track extending the length of the building. The wake-generating aircraft model is blade mounted on a strain-gage balance beneath a streamlined powered carriage, which travels along the overhead track. The support blade is adjustable to permit variation in model attitude. The model aircraft is towed at constant velocity through a test-section enclosure which serves to isolate the carriage wake from the model. The model used in the present investigation is shown exiting the test-section enclosure in the photograph in figure 2. The test section is 91 m long, 5.5 m wide, and 5.2 m high, with a 5-cm-wide opening in the ceiling to allow the model support blade to pass. The overhead track extends 305 m ahead of the entrance to the covered area to permit the carriage to accelerate to test velocities up to 30 m/sec.

Model and Test Conditions

A three-view sketch and principal geometric characteristics of the 0.03-scale model used for tests are shown in figure 3. The model was equipped with leading- and trailing-edge flaps deflected for landing approach (30°/30°), and the landing gear was extended. The notation (30°/30°) has conventionally been used to indicate the nominal angles of deflection of inboard and outboard trailing-edge flaps for the landing configuration.

A sketch of the model depicting the lateral-control surfaces that were oscillated in the tests and plots of the surface angular deflections through one cycle for lateral-control oscillation are presented in figure 4(a). A photograph showing the control surfaces oscillated is presented in figure 4(b). The surface frequency of oscillation was a nominal 3.4 cycles/sec to correspond for constant Strouhal number to a full-scale frequency of about 1/4 cycle/sec. (Based on pilot comments during the flight tests described in ref. 2, slower oscillation frequencies (1/6 to 1/4 cycle/sec) appeared to produce more attenuation than faster frequencies.) In figure 4(a), the oscillations were approximately sinusoidal with the exception that the spoilers were limited to the full-scale maximum deflection of 45°. Note that only the three inboard spoiler segments over the outboard flap were oscillated, and that the spoilers were deflected 30° at the neutral condition. In addition to this case, to simulate lateral-control oscillation, a case was also investigated in which the surfaces on one wing were oscillated in phase with those on the other wing. This case is referred to herein as "symmetrical" surface oscillation to distinguish it from the case in figure 4 which is referred to as "asymmetrical" surface oscillation. The surfaces were oscillated by means of mechanical linkage which was located inside the model with the exception of small crank arms protruding under the wings to connect to the surfaces. This mechanical linkage was driven by a small electric motor located inside the model fuselage. In addition to these two oscillating cases,

symmetric fixed spoiler deflection (three inboard segments over outboard flap) was investigated as a comparison baseline.

Since the model was rigidly mounted on the support blade, it was not possible to simulate the bank-angle excursions induced by the lateral-control oscillations in the flight tests. Although the effects of these aircraft motions are not known, it is conjectured that they would probably further disorganize the wake. In addition, engine thrust was not simulated in the tests. However, past work (ref. 4) has shown that engine thrust on this configuration is effective in attenuating the wake vortex. For these reasons, the results of the present investigation are believed to be conservative.

The model flight path was approximately 1.7 m below the test-section ceiling, a distance determined from previous tests to be sufficient to avoid significant effects on the model lift characteristics. Model attitude was set for a nominal lift coefficient of 1.4, corresponding to the landing configuration, in trimmed condition for all configurations tested, and test speed was a nominal 30 m/sec, giving a test Reynolds number of approximately 4.7×10^5 based on the model mean aerodynamic chord.

Flow-Visualization Instrumentation and Presentation of Results

Wake-vortex systems generated by the model aircraft were studied with a two-dimensional flow-visualization technique developed for the facility. Kerosene smoke was injected into the test section in a screen generally confined to a plane perpendicular to the model flight path and illuminated with flood lights. The model was then propelled through the smoke; and the wake action, made visible by the smoke induced along the flow streamlines, was recorded photographically with motion and high-speed still cameras. The cameras were positioned below the model flight path and viewed downstream, facing the approaching model. A detailed description of this flow-visualization technique can be found in reference 5.

Results are presented herein as visual time histories of the wake characteristics recorded on still photographs taken in rapid sequence during the test runs. In the figures, the full-scale downstream separation distance x in km (n.mi.) corresponding to the time at which each photograph was taken is given under the photograph, and the wake at increasing downstream distances is seen by viewing successive photographs in each row in the figure from left to right. In several of the figures, the model is seen in the first photograph immediately after it has passed through the smoke screen. A qualitative estimate of the rotary motion in the wake can be made from these still photographs by noting the extent to which the smoke is organized into spiral patterns. However, if the wake vortices are diffused and little rotary motion remains, it is generally impossible to detect this motion in the photographs. It should be emphasized, therefore, that the following discussion of data figures is also based on study of motion film coverage of the test runs.

RESULTS AND DISCUSSION

In this section, the characteristics of the basic unattenuated wake are presented first for comparison, with the attenuated wakes discussed later. Effects on the wake of fixed spoiler deflection and of lateral control-surface oscillations, both asymmetric and symmetric, are then discussed. In each case, details of the wake roll-up process are presented first, followed by a discussion of characteristics after roll-up is complete. In addition, a comparison is made between the apparent

amount of vortex attenuation obtained with asymmetric oscillating surfaces and with deflected spoilers.

Basic Configuration (No Control Deflections)

The basic unattenuated wake system is presented in the photographs in figure 5. As is well known from previous investigations (see ref. 6), initially separate vortices are shed on each side of the wake from the flap edges and wing tip. The dominant vortex is shed from the outer edge of the outboard flap, and weaker vortices are shed from the wing tip and inboard flap. The weaker vortices rapidly orbit about and merge downstream with the outboard-flap vortex (within a longitudinal travel of the aircraft of approximately 6 spans). After this point, the roll-up process is considered complete, and the wake system consists of two strong, persistent, counter-rotating vortices, which are characterized by apparently laminar cores and large maximum rotational velocities (ref. 7).

Because the wing-tip and inboard-flap vortices are relatively weak and merge rapidly with the outboard-flap vortex, it is difficult to see details of this roll-up process in figure 5(a). The positions of the individual vortices are identified in the photographs, however. Once roll-up is complete, a symmetric vortex with a well-defined core can be seen (note vortex from the port side of the model; core details of starboard vortex are not visible because of inadequate smoke seeding in this particular test run). As shown in figure 5(b), this vortex system persists, descending in the test section until it dissipates due to its close proximity to the test-section floor at a full-scale downstream distance of about 3 n.mi.

Effects of Fixed Spoiler Deflection

The effects of deflected flight spoilers on the wake characteristics are shown in the photographs in figure 6. This wake system differs considerably from the basic wake in terms of initial vorticity distribution, roll-up dynamics, and characteristics after roll-up. Roll-up (fig. 6(a)) is characterized by a strong vortex pair shed from the inboard flap, and a relatively weak, diffused vortex system shed from the outboard flap and wing tip. The inboard-flap vortex pair is shed in the strong downwash field behind the flap, descends rapidly below, and then orbits outward from the wing-tip and outboard-flap system ($x = 0.23$ n.mi.). These two vortex systems slowly merge ($x = 0.52$ n.mi.), a process taking a full-scale downstream distance of approximately 1 n.mi. to complete. Unlike the basic vortex, once roll-up is complete, this system consists of a diffused region of rotating flow without a well-defined core.

A better understanding of the effects of deflected spoilers on roll-up can be gained by a consideration of their expected influence on both the local flow region over the outboard flap and, more generally, on the overall wing spanwise lift distribution. Due to the action of the spoilers, much of the flow over the outboard flap would be separated, reducing the flap loading and injecting turbulence into the vortex shed from its outer edge, both effects combining to weaken and diffuse this otherwise dominant vortex. Also important is the fact that a measured increase in angle of attack of about 2.5° was required to maintain the lift coefficient of 1.4 with these three spoiler segments deflected 45°. The resulting increased lift inboard would be expected to increase the strength of the inboard-flap vortex and the downwash velocity behind the flap. In addition, since the lift carryover to the outboard flap would be reduced, the spanwise lift gradient between the flaps would become more

pronounced and result in a stronger vortex from the outboard edge of the inboard flap, creating a vortex pair from this flap. These combined effects result in the trailed vorticity behind the wing being redistributed into three separate regions, which subsequently become further separated because of the large difference in downwash behind the two flap systems. With the total vorticity now more equally divided into these widely separated regions, roll-up is delayed, allowing diffusion of vorticity to occur, particularly in the vortex pair as it spreads while merging.

Beyond a downstream separation of 1 n.mi., however, a more organized vortex system forms, with a visible core region (fig. 6(b)). This system descends somewhat more slowly than the basic wake, permitting observation to a greater downstream distance. For the downstream distance of approximately 4 n.mi. shown in figure 6(b), the vortex system persists with little apparent further decay.

Effects of Asymmetric Surface Oscillation

A particularly valuable feature of the flow-visualization technique employed is that it permits observation of wake flow nonuniformities and vortex interactions. In the present tests, control-surface oscillation produced large longitudinal flow nonuniformities in the wake during each cycle of oscillation. Use of this technique to analyze the wake with such periodic flow disturbances, however, required study of numerous test runs for a given configuration. The time history of only one two-dimensional region in the wake could be observed on a given test run, and the two-dimensional wake characteristics differed greatly within the longitudinal region represented by each period of oscillation. In other words, the wake characteristics seen on a given test run depended on the phase of oscillation, that is, the orientation of the control surfaces as the model aircraft passed through the smoke screen.

For the asymmetric oscillating case presented in figure 7, two longitudinal regions with distinctly different characteristics were observed, one asymmetric and one symmetric. Roll-up of the asymmetric region (fig. 7(a)) is characterized initially by a stronger, more defined vortex on one side of the wake than on the other. (See wake from port side of the model in fig. 7(a) at $x = 0.27$ n.mi.) This vortex system is shed from the wing-tip and outboard-flap outer-edge vortex (vortex system (2)). As roll-up continues, however, rotation on this side diminishes rapidly, and by the time roll-up is complete (approximately 1 n.mi.), the wake is relatively symmetrical (see lower right photograph in fig. 7(a)). Either side of the wake can exhibit this greater rotation on different test runs, depending on surface orientation during passage of the model through the smoke screen. On the opposite side of the wake, the wing-tip and outboard-flap vortex system (vortex system (1)) is diffused with reduced rotation. A vortex pair is shed from the inboard flap on that side (vortex system (3)), descends well below and then outboard of this system ($x = 0.27$ n.mi.), and appears to dissipate without merging ($x = 0.49$ n.mi.).

An interesting additional roll-up characteristic of this asymmetric region is a lateral transfer of the inboard-flap vortex system from the stronger to the weaker side of the wake. Note that the port inboard-flap vortex pair (vortex system (4)) in figure 7(a) transfers to the other side of the wake and merges with the vortex systems on that side. This lateral transfer is shown clearly in figure 7(b) where the smoke screen is not as dense, permitting the individual vortex systems to be distinguished more easily. In figure 7(b), the stronger wing-tip and outboard-flap vortex system is seen on the starboard side (vortex system (3)), and it is the starboard inboard-flap vortex pair (vortex system (1)) that transfers. Note that the lateral transfer occurs in a relatively short period of time, being essentially complete

within a downstream distance of approximately 0.25 n.mi. This vortex transfer is thought to result from the fact that the centroid of the wake vorticity is not coincident with the wake centerline when the surfaces are deflected asymmetrically, since the total lift on the wings is unequal.

Final roll-up of the three vortex systems making up the weaker side of the wake takes a downstream distance of approximately 1 n.mi. A broad region of turbulent flow is produced that exhibits practically no rotary motion once the merging process is complete. (See vortex systems (1), (3), and (4) at $x = 0.87$ n.mi. in fig. 7(a).)

Characteristics of the asymmetric region beyond a downstream distance of 1 n.mi. are shown in figure 7(c). The small amount of rotary motion remaining in the wake on the stronger side (wake from port side of model in fig. 7(c)) continues to rapidly diminish so that after a short distance farther downstream, practically no rotary motion is observed on either side of the wake in this asymmetric region (see photograph at $x = 1.30$ n.mi.).

Roll-up of the symmetric region (see fig. 7(d)) is characterized by a strong inboard-flap vortex pair and a relatively weak, diffused wing-tip and outboard-flap vortex system on each side. The inboard-flap system decends below and then outboard of the wing-tip and outboard-flap system (photographs at $x = 0.26$ and 0.49 n.mi.), merging with it at a downstream distance of approximately 1 n.mi. (lower right photograph). At this downstream distance, a moderate amount of rotary motion remains in the wake. Farther downstream (see fig. 7(e)), this rotary motion diminishes, but a small amount is seen to remain in this symmetric region ($x = 1.48$ n.mi.).

The symmetric regions are apparently produced when the lateral-control surfaces pass through the neutral setting, and the asymmetric regions are produced during other portions of the cycle, with the degree of asymmetry depending on the amount of surface deflection from neutral. Therefore, both symmetric and asymmetric regions are produced twice during each cycle. In the asymmetric regions, the stronger or weaker rotation is produced first on one side of the wake and then on the other, depending on whether the surface deflections correspond to a right or left control input. Therefore, the inboard-flap vortex systems transfer across the wake centerline from the stronger to the weaker side also twice each cycle; they transfer first from one side of the wake, then from the other, so the direction of transfer alternates. These large periodic movements of the inboard-flap vortex systems laterally across the wake are believed to be an important contributing mechanism to the rapid vortex breakdown observed for this asymmetric oscillating case.

A comparison between this wake, showing both asymmetric and symmetric longitudinal regions, and the wake with spoilers deflected 45° is presented in figure 8. This comparison indicates that asymmetric control-surface oscillation apparently produces a more disorganized wake with less rotary motion than is obtained with static spoiler deflection. Whereas the vortex system of the spoiler configuration (fig. 8(a)) appears to reform with a visible core region ($x = 1.49$ n.mi.) and to persist farther downstream ($x = 2.53$ n.mi.), the vortex system of the oscillating case is disorganized with reduced rotary motion at a downstream distance of approximately 1.50 n.mi. (figs. 8(b) and 8(c)).

Effect of Symmetric Surface Oscillation

In order to gain further insight into the flow mechanisms contributing to the vortex attenuation observed with asymmetric oscillation, tests were made with the

control surfaces oscillating symmetrically, a case for which vortex transfer across the wake centerline would not be expected. These tests differed from the asymmetric case only in that the control surfaces on one wing were oscillated in phase with those on the other wing.

Typical roll-up characteristics and subsequent wake development for this symmetric case are shown in the photographs in figure 9. As expected, the wake is symmetric, and no vortex transfer across the centerline is observed. Roll-up is characterized by a strong inboard-flap vortex pair that descends below (x = 0.14 n.mi.) and then outboard (x = 0.48 n.mi.) of the wing-tip and outboard-flap vortex system, merging with it at a downstream distance of approximately 1 n.mi. Farther downstream (x = 1.50 n.mi.) a more organized vortex system forms with a visible core region. Note that these wake characteristics are generally similar to those seen with the static deflected spoiler case (compare with fig. 6), and that the amount of vortex attenuation obtained is noticeably less than was obtained with asymmetric oscillation (compare with fig. 7). These results further indicate that the vortex transfer across the wake centerline that was observed with asymmetric oscillation may be an important vortex attenuating mechanism for that case.

CONCLUDING REMARKS

A flow-visualization study has been conducted in the Langley Vortex Research Facility to investigate effects of lateral control-surface oscillations on the wake of a 0.03-scale model of a wide-body jet transport aircraft. Effects of both asymmetric surface oscillation (control surfaces move as with normal lateral-control inputs) and symmetric surface oscillation (control surfaces move in phase) were compared to effects of fixed deflected flight spoilers. The asymmetric case simulated a flight maneuver which was previously investigated on the transport aircraft during NASA/FAA flight tests and which resulted in substantial wake-vortex attenuation. The following conclusions are drawn:

1. The simulated flight maneuver produced a more disorganized wake with less apparent rotary motion than was obtained with either symmetric surface oscillation or fixed deflected flight spoilers. For this asymmetric case, only a small amount of rotary motion remained in the wake-vortex system once roll-up was complete, a finding consistent with results of the flight tests.

2. Effects of surface oscillation on the vortex roll-up process were complex. With asymmetric oscillation, asymmetric regions were produced wherein part of the vortex system transferred across the wake centerline, merging with the vortex systems on the other side of the wake. This vortex transfer phenomenon is identified as a possible aerodynamic mechanism contributing to the large amount of attenuation observed with asymmetric oscillation.

3. Wake roll-up both for oscillating control surfaces and for fixed deflected spoilers was not complete for a full-scale downstream distance of approximately 1 n.mi.

Langley Research Center
National Aeronautics and Space Administration
Hampton, VA 23665
March 28, 1983

REFERENCES

1. Wake Vortex Minimization. NASA SP-409, 1977.

2. Barber, Marvin R.; and Tymczyszyn, Joseph J.: Wake Vortex Attenuation Flight Tests: A Status Report. 1980 Aircraft Safety and Operating Problems, NASA CP-2170, Part 2, 1981, pp. 387-408.

3. Croom, Delwin R.: Low-Speed Wind-Tunnel Parametric Investigation of Flight Spoilers as Trailing-Vortex-Alleviation Devices on a Transport Aircraft Model. NASA TP-1419, 1979.

4. Patterson, James C., Jr.; and Jordan, Frank L., Jr.: Thrust-Augmented Vortex Attenuation. Wake Vortex Minimization, NASA SP-409, 1977, pp. 251-270.

5. Patterson, James C., Jr.; and Jordan, Frank L., Jr.: A Static-Air Flow Visualization Method To Obtain a Time History of the Lift-Induced Vortex and Circulation. NASA TM X-72769, 1975.

6. Patterson, James C., Jr.: Vortex Attenuation Obtained in the Langley Vortex Research Facility. J. Aircr., vol. 12, no. 9, Sept. 1975, pp. 745-749.

7. Gartrell, Luther R.; and Rhodes, David B.: A Scanning Laser-Velocimeter Technique for Measuring Two-Dimensional Wake-Vortex Velocity Distributions. NASA TP-1651, 1980.

Figure 1.- Sketch of Langley Vortex Research Facility.

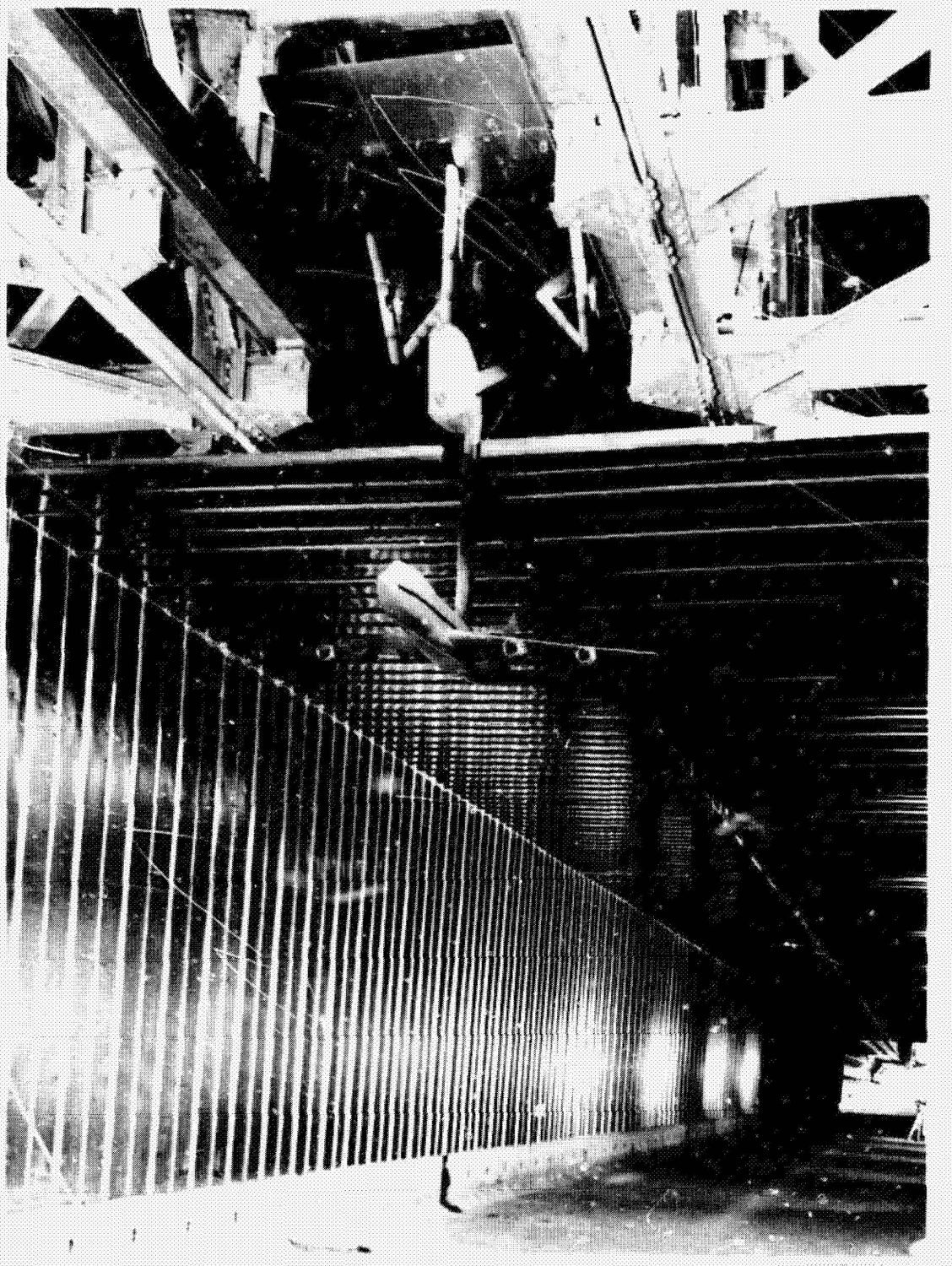

L-83-57

Figure 2.- Transport aircraft model exiting facility test section.

Wing	
Span, m	1.79
Mean aerodynamic chord, m	0.25
Root chord, m	0.497
Tip chord, m	0.121
Sweepback at quarter chord, deg	37.5
Area, m^2	0.460
Aspect ratio	6.96
Fuselage	
Length, m	2.06
Horizontal tail	
Span, m	0.664
Area, m^2	0.123
Aspect ratio	3.6

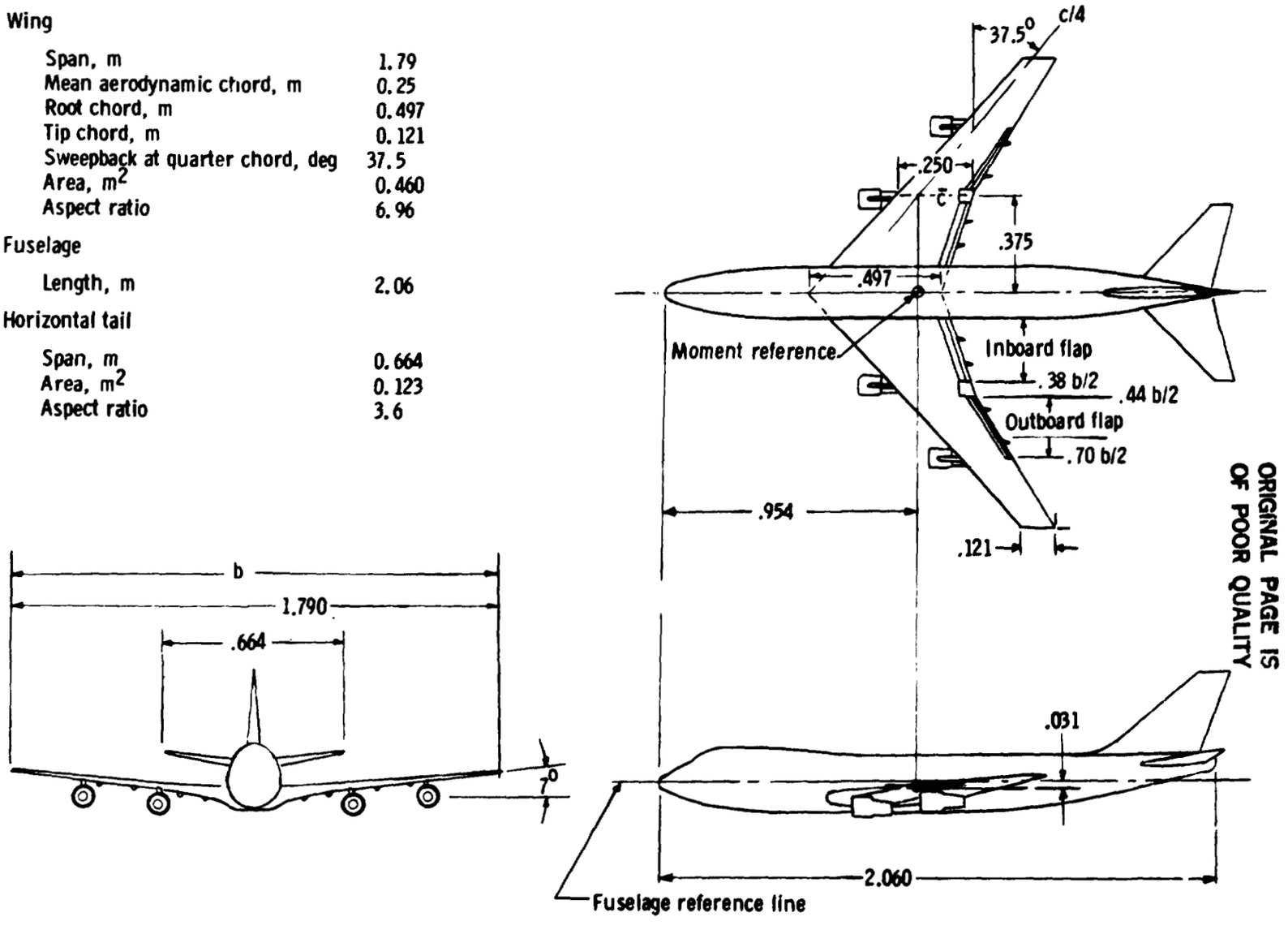

Figure 3.- Three-view sketch of transport aircraft model used in tests. Linear dimensions are in meters.

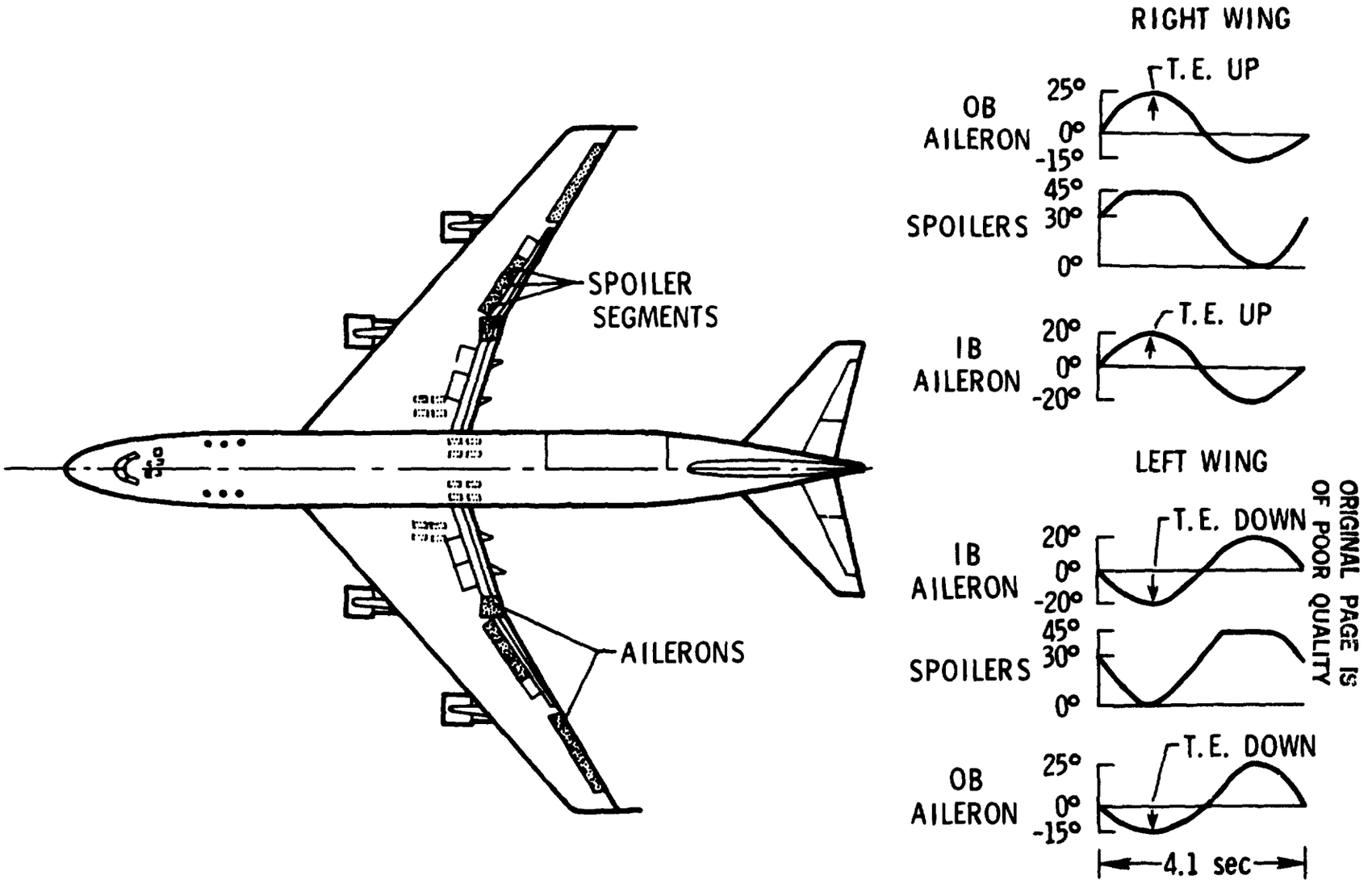

(a) Sketch showing surfaces oscillated on model and plots of surface angular orientation through one cycle for asymmetric case.

Figure 4.- Oscillating lateral-control surfaces.

(b) Photograph showing control surfaces oscillated on model.

Figure 4.- Concluded.

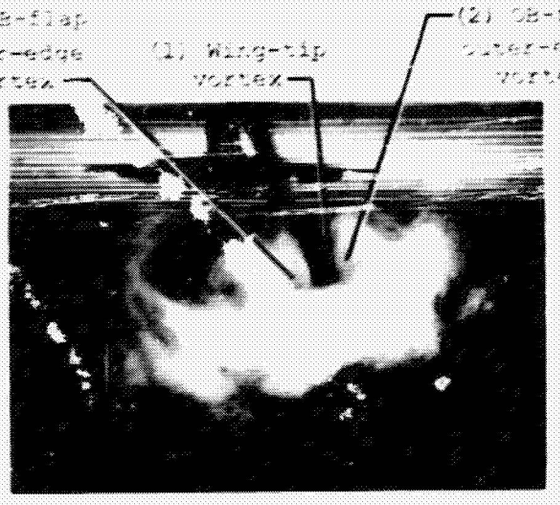

x = 0.13 (0.07)

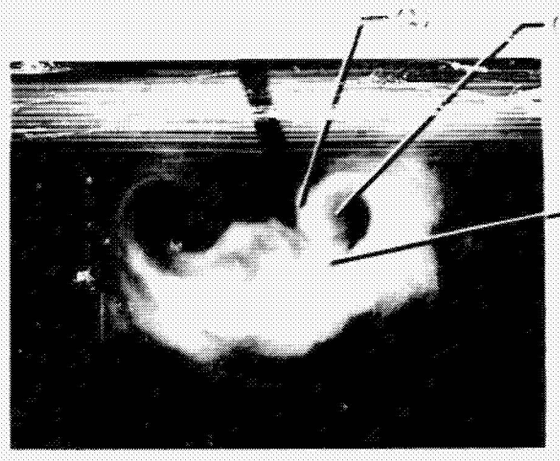

x = 0.27 (0.14)

x = 0.38 (0.21)

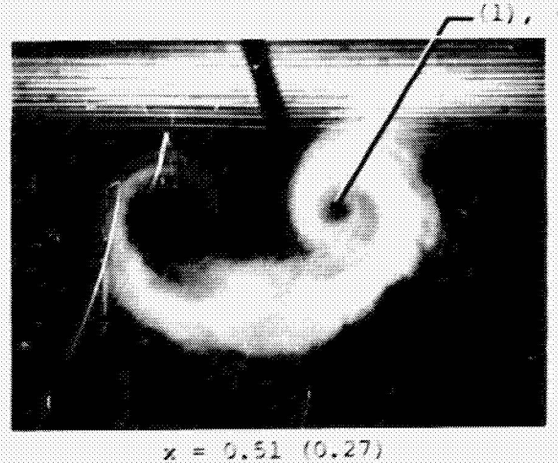

x = 0.51 (0.27)

(a) Roll-up. C_L = 1.41.

L-83-58

Figure 5.- Unattenuated wake-vortex system of landing approach configuration (flaps 30°/30°). Downstream separation distance x is given in km (n.mi.).

(b) Complete history. C_L = 1.36.

L-83-59

Figure 5.- Concluded.

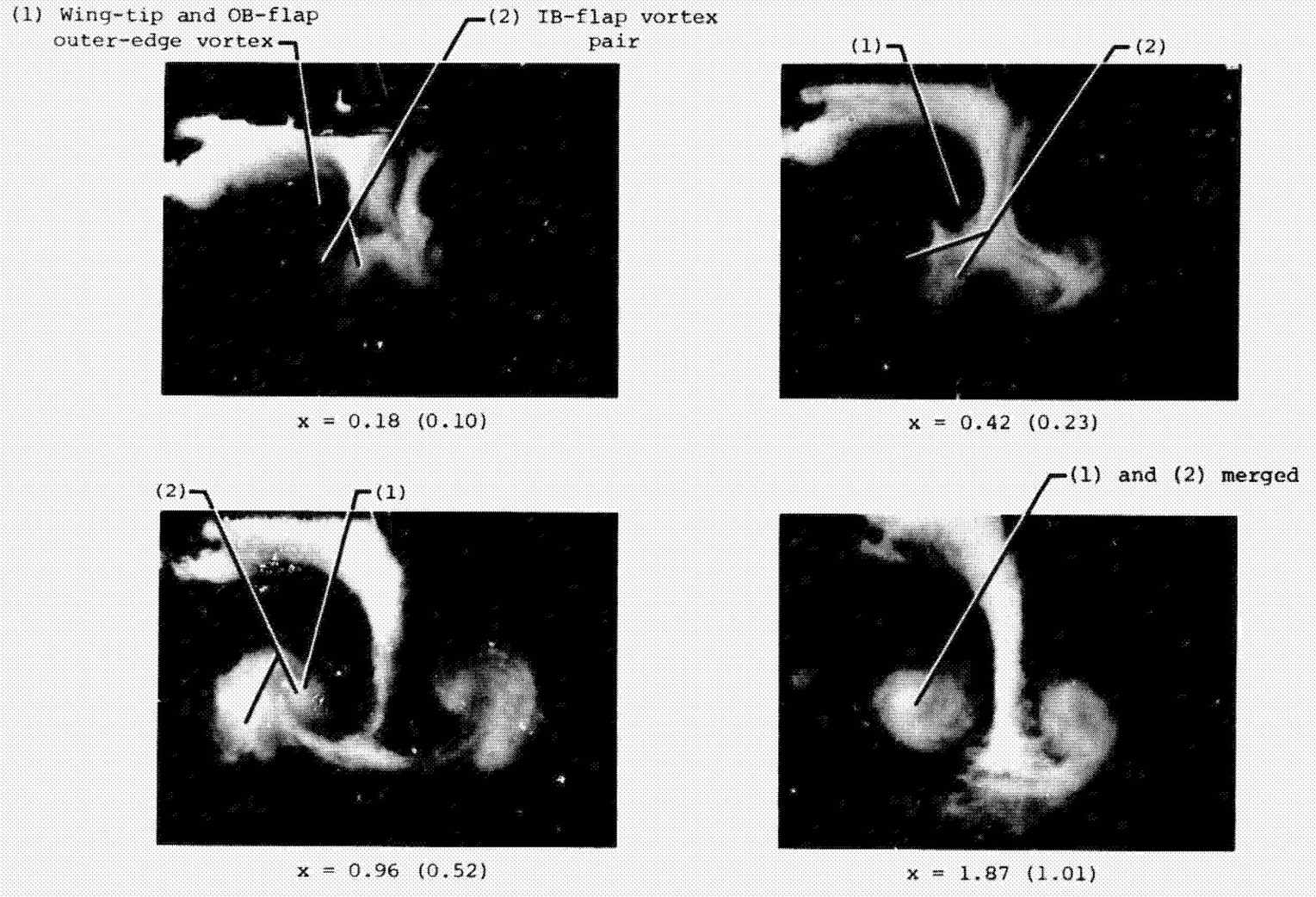

(a) Roll-up.

L-83-60

Figure 6.- Effects of deflected flight spoilers on wake characteristics. Spoiler deflection angle = 45°. C_L = 1.36. Downstream separation distance x is given in km (n.mi.).

(b) Complete history.

Figure 6.- Concluded.

L-83-61

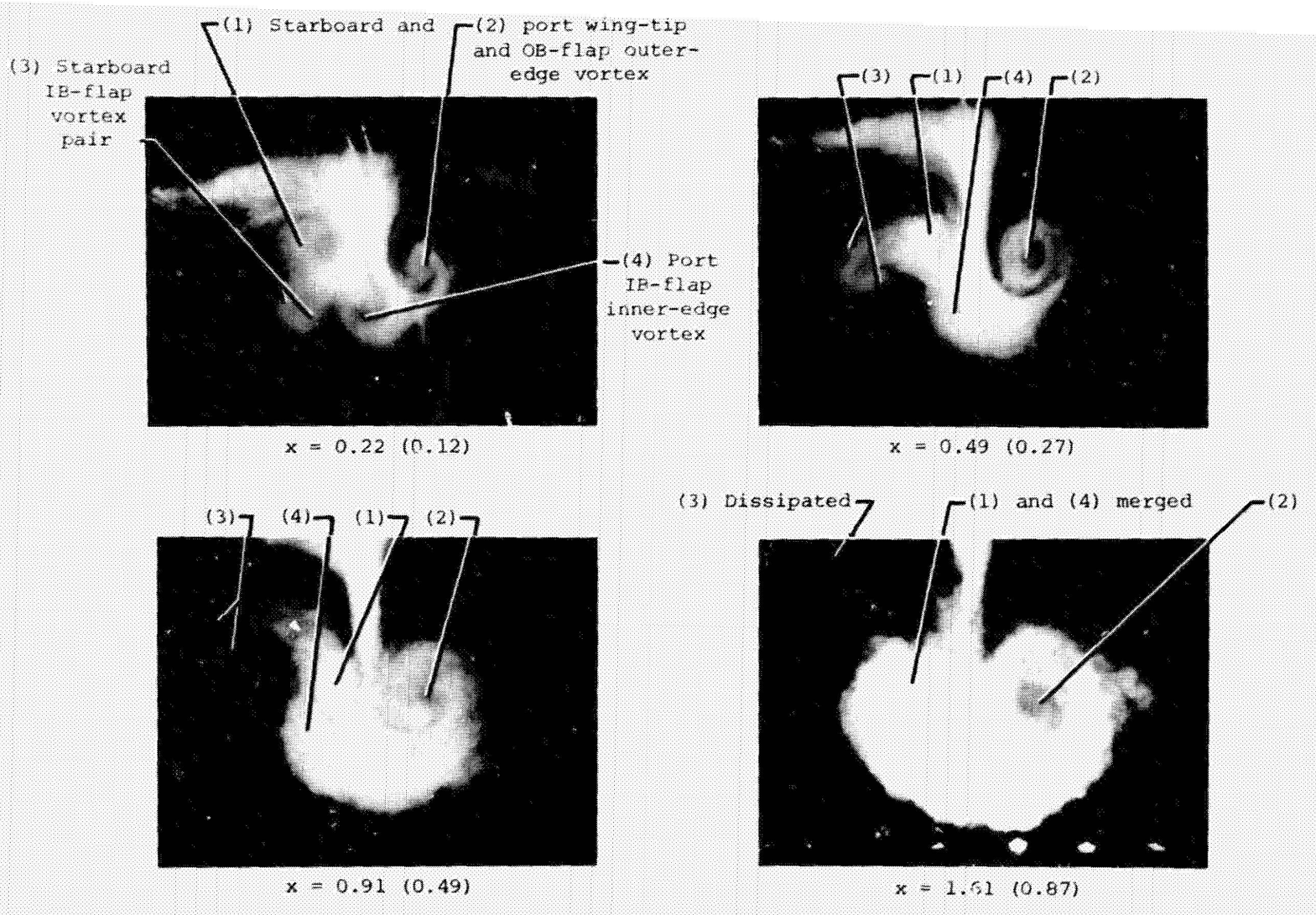

(a) Roll-up of asymmetric longitudinal region. C_L = 1.41.

L-83-62

Figure 7.- Effects of asymmetric control-surface oscillation on wake characteristics. Frequency of oscillation = 3.4 cycles/sec. Downstream separation distance x is given in km (n.mi.).

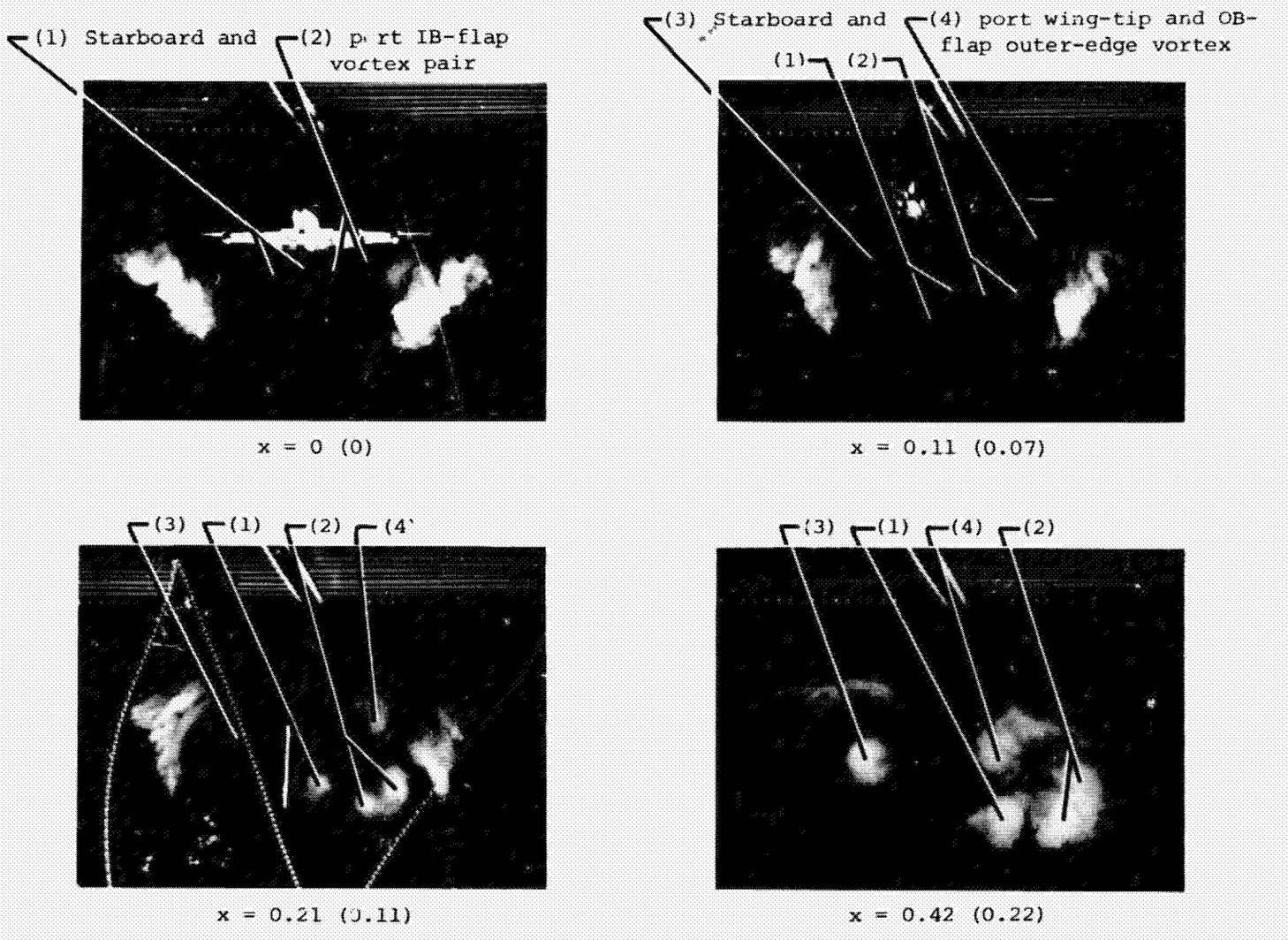

(b) Roll-up of asymmetric longitudinal region showing lateral transfer of vortex pair shed from inboard flap. C_L = 1.40.

L-83-63

Figure 7.- Continued.

x = 1.59 (0.86)

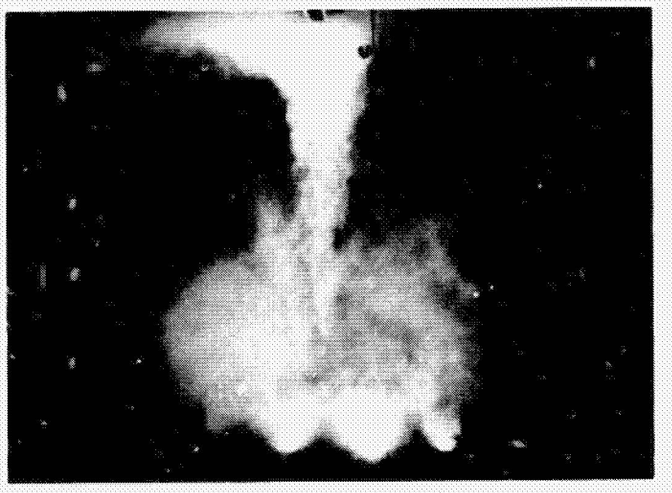

x = 2.40 (1.30)

x = 3.21 (1.73)

x = 4.69 (2.53)

(c) Complete history of asymmetric longitudinal region. C_L = 1.36.

L-83-64

Figure 7.- Continued.

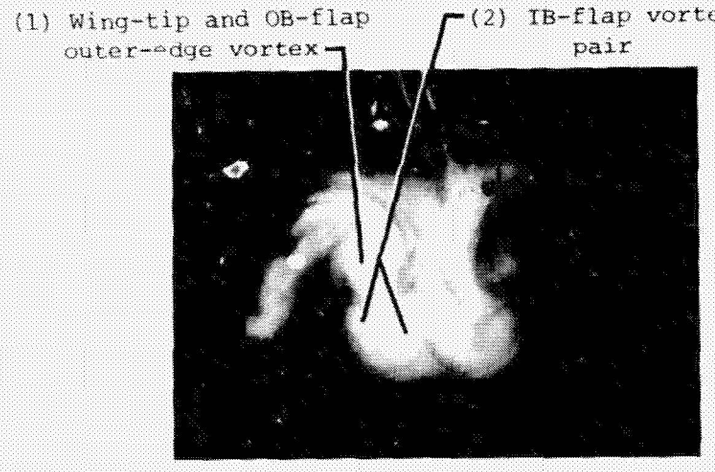

x = 0.21 (0.11)

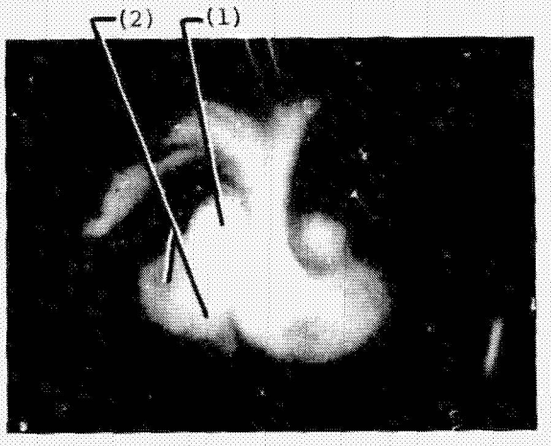

x = 0.47 (0.26)

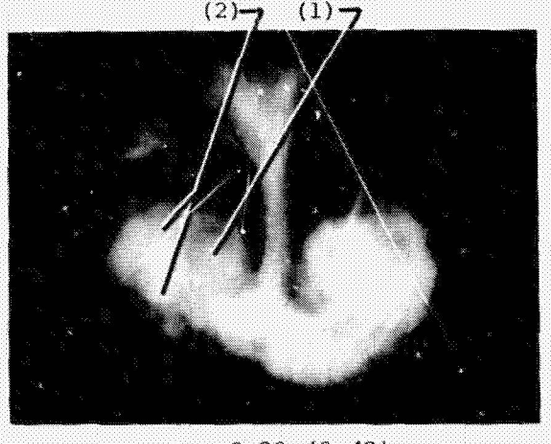

x = 0.90 (0.49)

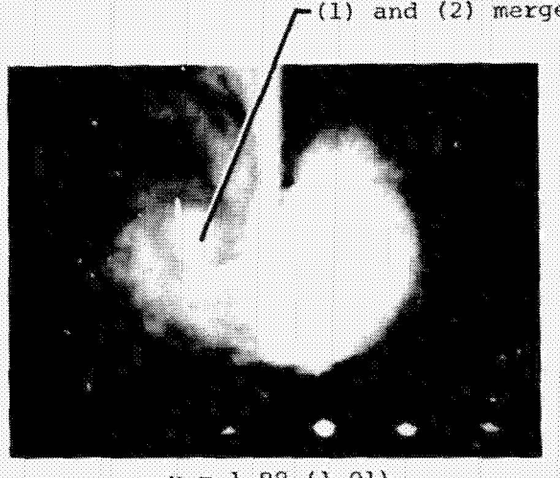

x = 1.88 (1.01)

(d) Roll-up of symmetric longitudinal region. C_L = 1.42.

L-83-65

Figure 7.- Continued.

x = 1.80 (0.97)

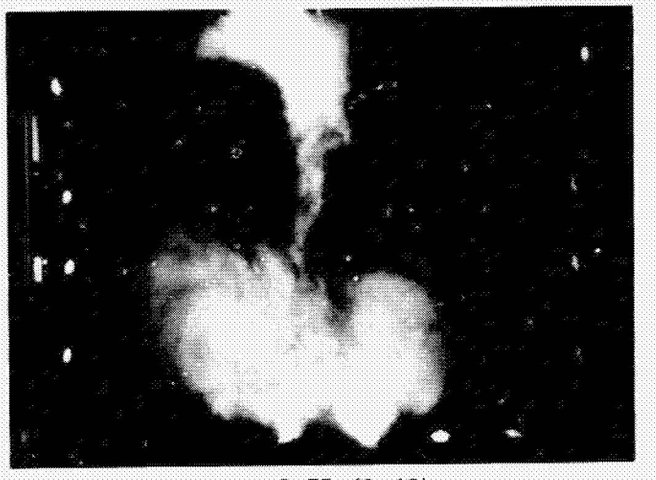

x = 2.75 (1.48)

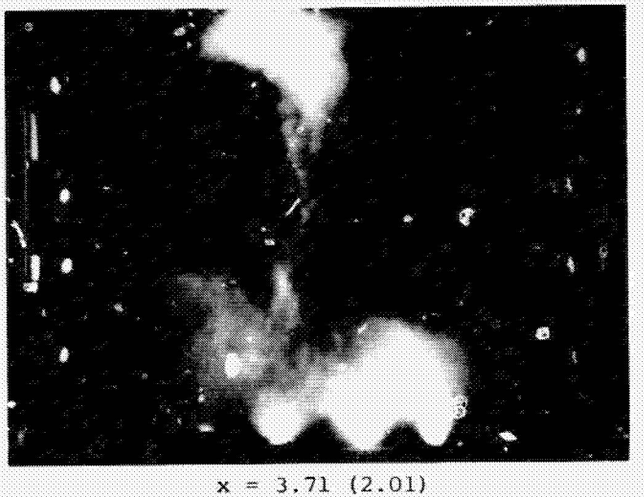

x = 3.71 (2.01)

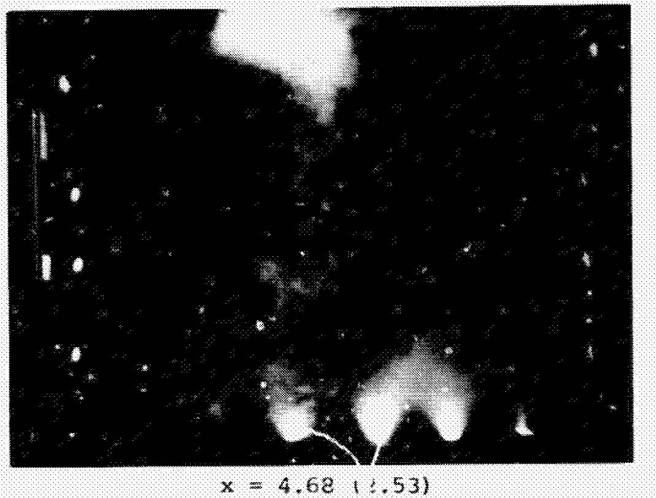

x = 4.68 (2.53)

(e) Complete history of symmetric longitudinal regio 1.39.

L-83-66

Figure 7.- Concluded.

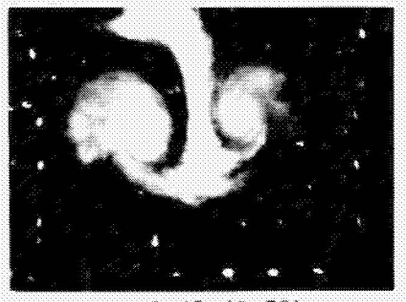

x = 1.45 (0.78)

x = 2.77 (1.49)

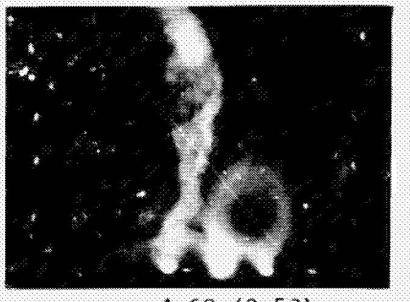

x = 4.68 (2.53)

(a) Spoilers deflected 45°. C_L = 1.36.

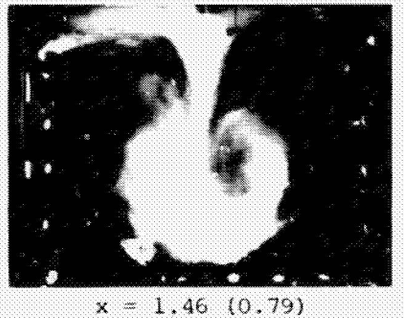

x = 1.46 (0.79)

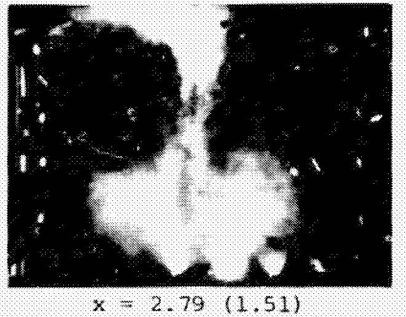

x = 2.79 (1.51)

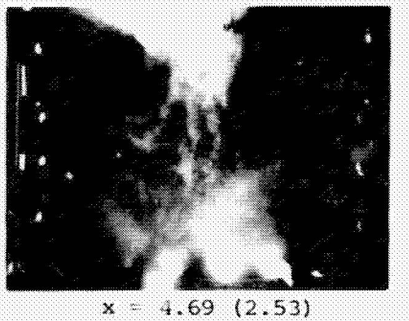

x = 4.69 (2.53)

(b) Oscillating case showing asymmetric longitudinal region. C_L = 1.36.

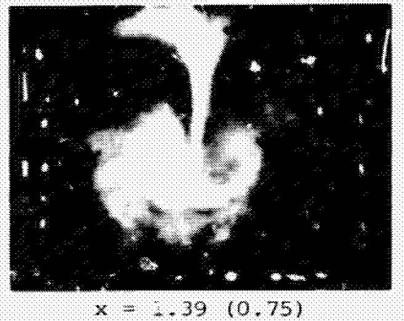

x = 1.39 (0.75)

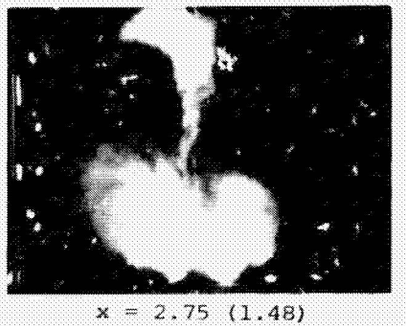

x = 2.75 (1.48)

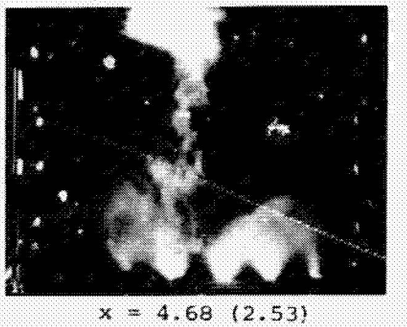

x = 4.68 (2.53)

(c) Oscillating case showing symmetric longitudinal region. C_L = 1.39.

L-8[illegible]

Figure 8.- Comparison between wake characteristics of spoiler and asymmetric oscillating configurations. Frequency of oscillation = 3.4 cycles/sec. Downstream separation distance x is given in km (n.mi.).

x = 0.26 (0.14)

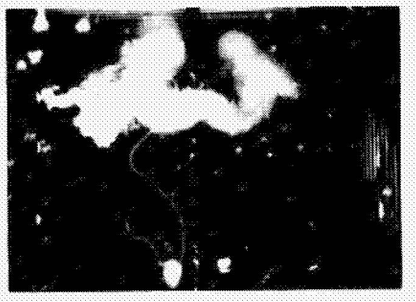

x = 0.39 (0.21)

x = 0.64 (0.35)

x = 0.89 (0.48)

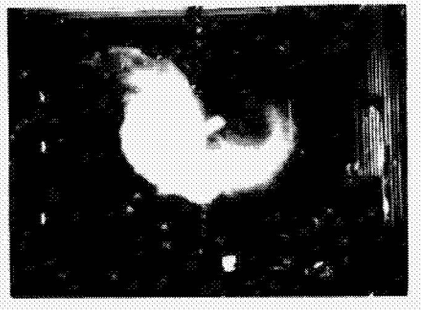

x = 1.90 (1.03)

x = 2.78 (1.50)

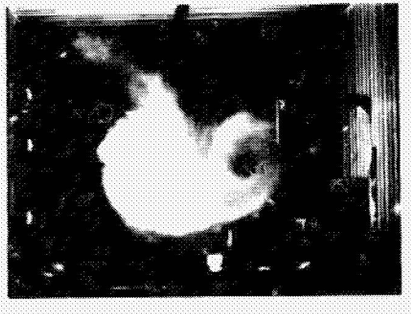

x = 3.29 (1.78)

x = 3.65 (1.97)

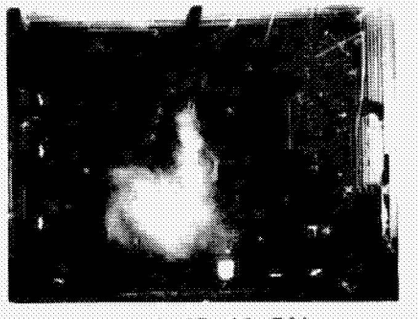

x = 4.65 (2.51)

L-83-68

Figure 9.- Effects of symmetric control-surface oscillation on wake characteristics. Frequency of oscillation = 3.4 cycles/sec. Downstream separation distance x is given in km (n.mi.).